Journal of Solid Mechanics Vol. 14, No. 4 (2022) pp. 499-513
DOI: 10.22034/jsm.2022.1926526.1688

Research Paper

Numerical and Experimental Analysis of Impact and Damage on Composite Sandwich Panels with Grid-Stiffened Core

J. Faraji Shoaa[1], A.Davar [2,*], J.Eskandari Jam [2], M. Heydari Beni [2]

[1]*Department of Mechanical Engineering, Malek ashtar University of Technology, Tehran, Iran*
[2]*Faculty of Materials and Manufacturing Technologies, Malek Ashtar University of Technology, Tehran, Iran*

Received 8 August 2022; accepted 10 October 2022

ABSTRACT

A composite grid sandwich panel consists of a core with a composite grid structure and two faces on both sides of the core. This study investigated low-velocity impact in grid sandwich panels with grid cores experimentally and numerically by constructing and performing experimental tests using Abaqus finite element software. In the experimental part, three sandwich panels with grid cores were made for the low- velocity impact test. In the numerical part, three-dimensional elements were used, and damage was solved via programming in the Fortran language in Abaqus software. The results showed that the use of foam in the core of these structures reduced deflection due to impact despite a slight increase in the final weight of the structures.

Keywords : Impact and damage analysis; Sandwich panel; Composite grid core; Numerical and experimental methods.

1 INTRODUCTION

SANDWICH panels are commonly used in many engineering structures, such as aerospace and aircraft structures, marine structures, and turbines. In these structures, most of the bending and membrane forces are carried by the faces, and shear loads are transferred by the faces to the core. Although the lightweight of composite structures and sandwich panels is beneficial, the damage to them due to impact strongly reduces their hardness, stability, and load-carrying capacity. Flying debris and small objects on airport runways due to the movement of airplane wheels during take-off and landing are among impactors. Moreover, the internal damage caused by impact in these structures is hardly detected in technical inspections [1, 2]. Yang et al. numerically and experimentally studied an aramid/epoxy composite panel of various thicknesses under different energies subjected to low-velocity impact. The experimental results showed that the impactor energy had a significant effect on the contact force history, such that the force-time graph was smooth and nearly-sinusoidal when the impactor energy was low, while an increase in the impactor energy caused high fluctuation in the graph and a sudden drop to occur in the graph after the maximum contact force [3]. Crupi et al. [4] compared the impact-resistance of an aluminum sandwich panel with that of a sandwich panel with a composite face and foam core. Wang et al. [5] performed experimental and

*Corresponding author. Tel.: +98 21 22945140.
E-mail address: a_davar@mut.ac.ir (A. Davar)

numerical low-velocity impact tests on sandwich panels made of carbon/epoxy faces and cores filled with polyurethane foam with different impactor energy levels, face thicknesses, and cores. Some of their results are as follows:

1. The impact parameters, such as maximum force, the ratio of absorbed energy to impact energy, and contact time increased with a rise in the impactor energy. Also, the absorbed energy to impact energy ratio and contact time decreased with the impactor size, while the maximum contact force increased with it.
2. The damage level and indentation depth increased with a rise in the impactor energy but decreased with an increase in the face thickness.
3. The impact response and the damage condition were independent of the core foam thickness.
4. Most often during an impact, the foam core was first destroyed by approaching a constant contact force; then, the contact force gradually increased. The presence of the foam reduced advances in fiber and matrix fracture in the shell [6].

Soroosh et al. numerically studied low-velocity impact on a multi-layer composite panel. By investigating the impactor parameters, they found out that by considering constant kinetic energy for the impactor, the maximum contact force first increased with a rise in velocity, but the increase rate of the maximum contact force became very small from a specific velocity onward. In addition, the coefficient of restitution first decreased and then increased with an increase in the impactor radius [7]. Azarafza et al. experimentally investigated the three-point bending test of a metal and composite sandwich panel with a grid core and demonstrated that the grid core continued to bear the load even after the faces yielded. They also showed that changing the material of the faces from fabric with glass fibers to carbon produced better results in sandwich structures than increasing the thickness of glass fiber faces [11]. Keramat Malekzadeh et al. presented an analytical model for predicting the dynamic response of a sandwich panel with top and bottom layers made of fiber-metal under low-velocity impact. They observed that a rise in the impact resistance of the structure was independent of the impactor velocity and mass at constant energy. Furthermore, with a drop in the thickness of layers in sandwich structures, the maximum impact force-indentation curve approached a linear state [12]. Aryal et al. investigated the effects of impact energy, velocity, and impactor mass on the damage induced in composite laminates and sandwich panels. They employed the microscopic non-intrusive damage assessment procedures to investigate various damage modes induced by the drop weight impact depending on the impact of velocities and impactor masses [13]. Zhu et al. studied the dynamic response of foam core sandwich panel with composite facesheets during low-velocity impact and penetration. They compared predictions with experimental and numerical results and achieved reasonable agreement. Their work provides an analytical method to study the mechanisms of impact damage and energy absorption for the composite sandwich panels with closed-cell foam core [14]. Najafi et al. designed a multilayered hybrid cored-sandwich panel stiffened by thin-walled lattice structure. They conducted a wide range of experimental tests including water immersion conditioning, three-point bending, edgewise and flatwise compression, quasi-static indentation, and high-velocity impact perforation to characterize the environmental durability and mechanical properties of the panel. The principal findings were that the proposed structural modifications caused a significant enhancement in all the studied mechanical and durability properties of PU foam-cored sandwich panels. It was also found that the FE model could predict load-displacement behavior of the studied sandwich panels under a variety of experimental conditions [15]. Sandwich panels with composite grid cores are new structures used in aerospace and other engineering applications. Grid structures in the cores of these panels increase their impact energy absorption capacity and prevent their total collapse. Previous research on low-velocity impact in sandwich panels generally focused on panels with honeycomb cores or specific core structures. Sandwich panels with composite grid cores have exhibited better performance than other types of sandwich panels in static loading. However, it is necessary to investigate their behavior against dynamic loads and impact to better understand these panels.

The present study investigated these panels experimentally and numerically using two approaches: building an all-composite sandwich panel with a grid core via newer methods and using accurate three-dimensional (3D) numerical models. The grid core of the sandwich panel was fabricated by manual filament winding with continuous fibers and simultaneous soaking, where continuous winding with tension in the fibers created a strong grid structure. The numerical model of this study present a model more realistic than two-dimensional models using 3D progressive damage models in composite materials and the coding capabilities of Abaqus software.

2 FABRUCATION METHOD

Glass fiber with the technical code Silenka Hoogezand-Holland (084-K28) and hot cured epoxy resin (Araldite ® LY 556/Hardener HY 917/Accelerator DY 070) were used to fabricate the sandwich panel cores. Also, glass fibers

were used in the form of unidirectional fabric to fabricate the sandwich panel faces, and the resin used in these layers was cold-cured epoxy.

Fig.1
The glass fiber used to fabricate the grid core.

The sandwich panel was built as follows: First, the grid core was fabricated using a special fixture and mold and fully cured in an autoclave. Then, the top and bottom faces were fabricated uniformly. Finally, the core and faces were attached using epoxy resin. The sandwich panel fabrication method is explained in detail in the following section. A silicone mold was prepared to build the grid core. To this end, it is necessary to first prepare a reference model with the final shape of the sandwich panel core. Plexiglas was used to make the reference model. The sandwich panel core was converted to a 3D model and cut from Plexiglas with the exact desired dimensions. The mold was prepared by placing the model inside a rectangular frame and using Silicone molding material. Plexiglas prepared for making the silicone mold is displayed in Fig. 2.

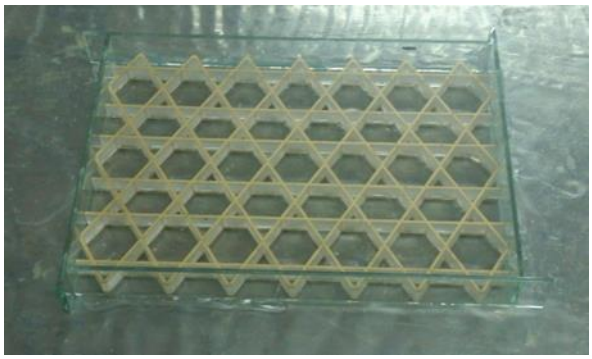

Fig.2
Plexiglas for making the silicone mold.

As shown in Fig. 2, the reference model was placed inside a rectangular frame. Then, the silicone molding material was mixed and poured into the frame so that the pores were well-filled. After the time required for curing silicone (24 hours), the reference model was removed. It was done easily due to the very low adhesion of silicone. The mold was used after several days so that the silicone was fully cured and the mold was strengthened. The silicone mold after the final preparation is shown in Fig. 3.

Fig.3
The silicone mold after the final preparation.

Since the grid core was made using continuous fiber, it was necessary to place a pin for winding at the end of each rib for continuous filament winding. For this purpose, a fixture was built according to Fig. 4. As shown in the figure, there was a pin along each rib. Pins were fixed on one side of this fixture and were placed on an adjustable

screw on the other side of the fixture. The adjustability of the screw at two sides made it possible for the fibers in the rib to come under tension by twisting the screws after filament winding.

Fig.4
Fixture for building the grid core.

The grid structure of the core was made manually via wet lay-up. For this purpose, after preparing the fixture and silicone mold, the manual winding process began from one side of the first rib, and the first layer was placed in unidirectional ribs continuously and via pulling by hand. The winding was performed first for the diagonal ribs and then for the horizontal ribs. Also, it is worth mentioning that the filaments used for winding were first fully soaked in a resin bath. For better soaking the filaments during the stay in the bath, the resin temperature was raised to 40°C using a heater. After the end of the grid core lay-up, the structure was placed in the autoclave along with its fixture under a curing cycle for 2 hours at 80°C and 3 hours at 140°C for the resin to be cured. This project aimed to fabricate three identical sandwich panels. Therefore, the shells of each panel was made after building the three grid cores. Three layers of unidirectional glass fibers were made with the required dimensions along with cold epoxy resin.

The layer was made with a hand lay-up with the order [0/90/0] on a clean glass surface. Then, the shells were attached to the core with cold epoxy. Sufficient time was provided for the full curing of the resin, and strong adhesion was made by placing weights on the layers. The sandwich panel after completion is shown in Fig. 5. The empty spaces of the core of one of the three sandwich panels were filled with hard foam. For this purpose, one of the faces was placed on this sandwich panel, and after it hardened, the empty spaces between the ribs were filled with hard foam. Two liquid foam constituents were used to fill the empty spaces between the ribs. By mixing these two constituents with a one-to-one ratio, the foam formed after a few seconds and filled the empty spaces within the core. After the core was filled with foam, the second face of the sandwich panel was similarly attached to the other panels, and the final sandwich panel was ready.

Fig.5
The sandwich panel after completion.

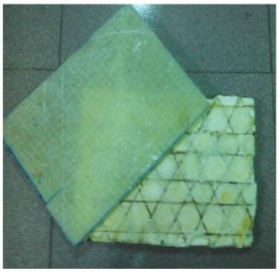

Fig.6
The sandwich panel with hard-foam-filled core.

3 EXPERIMENTAL FREE_FALL IMPACT TEST

After preparing the three sandwich panel samples, the free-fall impact test was performed on each of the panels. After placing the panels with the restraint in the test machine, closed with two clamps, vertical contact pressure was applied evenly on the surface edges of the panel. Some limitations of the impact test device were the maximum recordable acceleration (100*g*) and the maximum time to record information (26 milliseconds). The mass of the striker was multiplied by the measured acceleration to calculate the impact force.

The impact test was performed similarly for the three panels with the following parameters:

- Impactor mass: 11.6 *kg*
- Impactor height: 30 *cm*
- Impactor punch: spherical with a diameter of 16 *mm*

4 NUMERICAL SOLUTION OF IMPACT ON THE SANDWUCH PANEL

In this problem, the impactor with a mass of 11.6 *kg* and a spherical punch with a diameter of 16 *mm* fell from a height of 30 *cm* and collided with the fabricated composite panels. Then, the impact response was investigated.

The following assumptions were used in all the numerical solutions of this part:

- The impactor was considered to be a rigid spherical object, and all the masses belonging to the impact test device were considered an equivalent mass at the center of the sphere mass.
- The contact between the impactor and the sandwich panel was considered to be of the surface-to-surface type with a friction coefficient of 0.5.
- The gravitational force during the impact was ignored.
- The boundary conditions applied in the numerical analysis were considered based on the actual testing conditions.

4.1 Geometrical modeling of the sandwich panel

The sandwich panels examined in this study consisted of a grid core and faces. Based on the fabricated samples, the total length, width, and height of the panels were about 303 *mm*, 220 *mm*, and 21 *mm*, respectively. The two faces were 3 *mm* thick each, and the grid core took up 15 *mm* of the thickness of the sandwich panel.

The unit cell used to form the panel core is shown in Fig. 7.

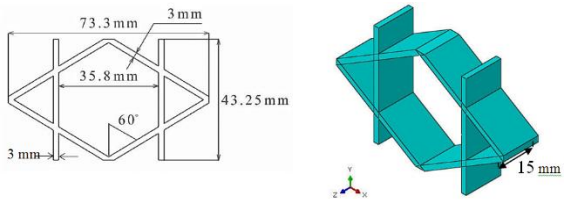

Fig.7
The dimensions of the constituent cell of the panel core.

After modeling the unit cell, the whole core was modeled by replicating the unit cell throughout the two-dimensional surface in a rectangular pattern. Fig. 8 displays the final and complete core.

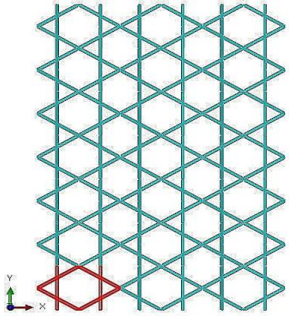

Fig.8
Modeling the sandwich panel core with in-plane replication of the unit cell.

The shells on the sides of the panel were modeled as a rectangular plane with the total length and height of the panel and a thickness of 3 *mm*, as shown in Fig. 9.

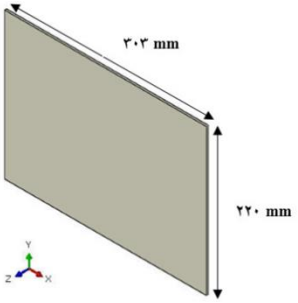

Fig.9
The shell used on the sides of the sandwich panel core.

The 3D foam filling the empty spaces of the grid core was modeled using CATIA software and imported to the Abaqus environment. The foam is shown in Fig. 10.

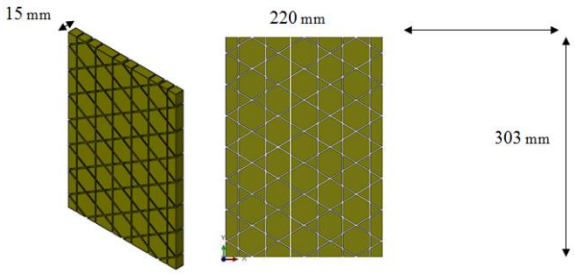

Fig.10
The three-dimensional model of foam used in the grid core (filling the empty spaces in the core).

As shown in Fig. 11, the impactor was in the form of a hemisphere with a diameter of 16 *mm*, and was modeled as a rigid body. It is worth mentioning that the modeled hemisphere was the geometry of the colliding part of the impactor, but the actual impactor consisted of parts and weights with known weights with a punch of the mentioned diameter at its end. However, the final impact load was exerted on the sandwich panel via this punch.

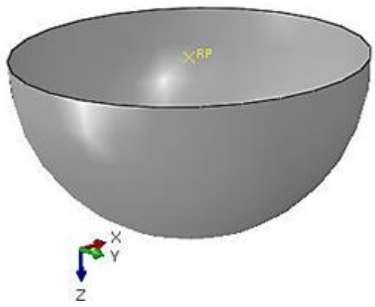

Fig.11
The spherical impactor.

It must be noted that since a velocity can be defined in Abaqus software for the impactor, there was no need for the impactor to be placed at the height where it was released, and the equivalent speed of the impactor at the instant of impact can be defined in other parts of the software.

4.2 Impact contact modeling

Surface-to-surface contact was considered to simulate the impact between the impactor and the sandwich panel. The contact along the tangent direction between the impactor and the sandwich panel was applied using the penalty command in Abaqus software, and a friction coefficient of 0.5 was selected according to [10]. Moreover, hard contact was selected for the normal direction between the impactor and the sandwich panel. For the shells of the sandwich panel, three layers of unidirectional fibers with [0/90/0] lay-up and properties according to Table 1 were

modeled. In case the shell element was used, all the three layers would be modeled together as an equivalent plate with the thickness of the three layers combined, and the order and direction of the layers would be assigned to the model using the software.

Table 1
The mechanical properties of the shells on the two sides of the sandwich panel

Strength		Elastic properties	
Xt (MPa)	450	*E1 (GPa)*	17.8
Xc (MPa)	283	*E2/ E3 (GPa)*	4.2
Yt (MPa)	24	*v12/ v13*	0.275
Yc (MPa)	80	*v 23*	0.38
SL (MPa)	21	*G12/ G13 (GPa)*	3.6
ST (MPa)	21	*G23 (GPa)*	2.2

The properties of the core ribs were determined as explained above. In case 3D elements were used, the direction of each rib would be determined individually, such that the fibers would be mainly directed along the rib directions, according to Fig. 12.

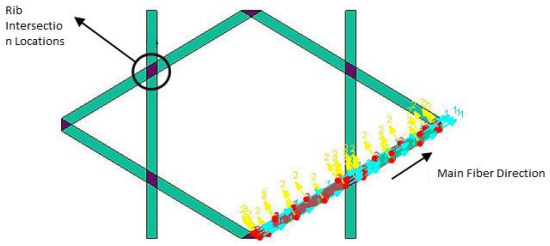

Fig.12
Determining the direction for assigning materials to the ribs.

Previous studies and experimental results have shown that the intersections of the ribs are weak compared to other points of grid structures, and fractures in static loading occur near the intersections [8]. According to Fig. 13, there was a region with high resin amounts near the rib intersections. This extra resin reduced the volume fraction of the fibers and led to a region with less stiffness and strength around the intersections.

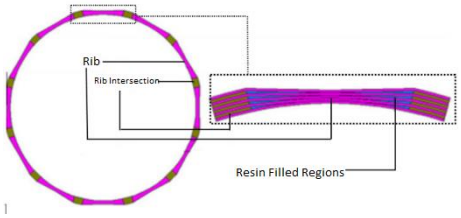

Fig.13
The schematic of the cross section of the grid cross section [8].

Accordingly, the mechanical properties of the rib intersections were considered to be 70% of those at the ribs in this study for a more realistic model. The properties used for the ribs are according to Table 2. It must be noted that the properties used for the shells and the ribs were extracted from previous experimental results and comparisons with existing references.

Table 2
The mechanical properties of the ribs [9].

Strength		Elastic properties	
Xt (MPa)	514	*E1 (GPa)*	22.5
Xc (MPa)	300	*E2/ E3 (GPa)*	7.63
Yt (MPa)	81.7	*v12/ v13*	0.22
Yc (MPa)	197	*v 23*	0.29
SL (MPa)	69	*G12/ G13 (GPa)*	2.37
ST (MPa)	69	*G23 (GPa)*	3.13

In addition, the properties of the foam used for the empty spaces in the core were based on its calculated density according to the following table.

Table 3
The mechanical properties of the foam used in the core.

ρ(kg/m3)	140
E (MPa)	180
Xt (MPa)	3.1
Xc (MPa)	2
ε (%)	2.37

4.3 Application of damage to the composite materials using subroutine programming

In the numerical simulation used in this study, 3D progressive damage relationships in composite materials with the help of Hashin's Theory were used for accurate solutions of the impact response. The fracture modes were investigated with subroutine programming in the Fortran language. It was possible for the subroutines to communicate during the solution execution in Abaqus software. In this program, the fracture modes were analyzed after the stresses were called. If any of the considered modes occurred, the material properties would change based on the fracture mode. The progressive damage model is shown in flowchart form in Fig. 14.

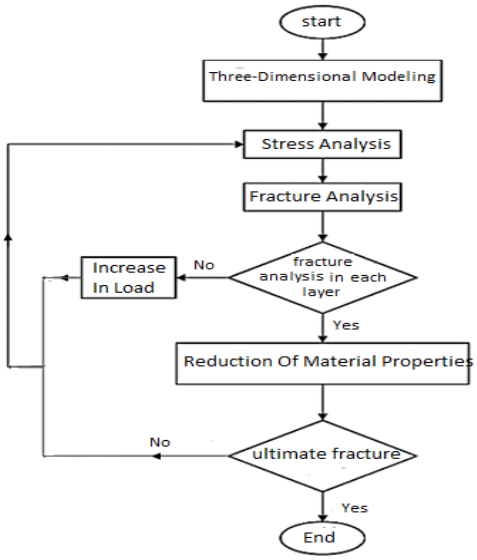

Fig.14
The flowchart of the progressive damage model.

4.4 Boundary conditions and loading

In this study, the only applied load was the free fall of an impactor with a known weight. As mentioned previously, it is possible to define the impact velocity of the impactor instead of placing the weight at a given height in the finite element analysis. Therefore, a speed equivalent to the release height (according to the relationship $V=\sqrt{2gh}$) was defined for the impactor along the collision direction.
According to experimental tests, the sandwich panel was placed in a fixture with internal dimensions 200mm×200mm for the impact test. As mentioned previously, the dimensions of the panels are about 303mm×220mm. By placing the panel in the fixture, a square of the mentioned dimensions in the middle of the panel was exposed to the impact, and the rest of the panel was between the top and bottom plates of the fixture. During the impact test, the bottom plate of the fixture was placed on the rigid plate of the device, and the top plate of the fixture held the plate tightly at two points using two clamps. In the numerical model, the sandwich panel and the fixture were modeled in the first step, and the boundary conditions were applied according to real conditions. The bottom plate was constrained, and also the top plate was constrained normal to the plane at two points. Moreover, contact was defined between the fixture and the sandwich panel. The modeling and the applied initial boundary conditions are displayed in Fig. 15.

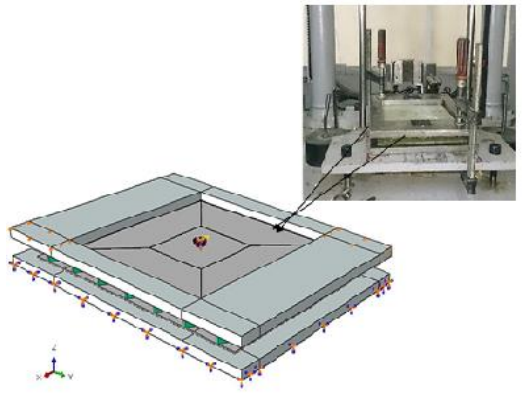

Fig.15
The application of boundary conditions in the numerical model according to the conducted experimental test.

In the subsequent step, for simplify the numerical solution and reduce the solution time, the fixture was eliminated from the model. For this purpose, parts of the bottom plate of the sandwich panel, placed inside the fixture, were constrained in all directions, and the top plate contacting the fixture was constrained along the direction normal to the plane. The boundary conditions applied in the finite element software are shown in detail in Fig. 16.

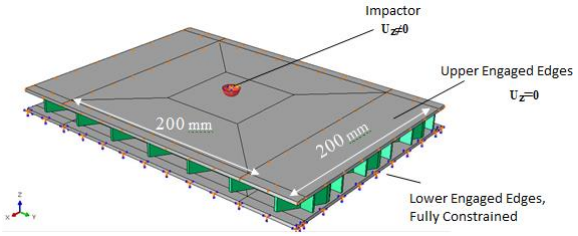

Fig.16
Details of the boundary conditions of the numerical model.

The preliminary analyses were performed on both boundary conditions, and the impact response results for the two boundary conditions were very close (Fig. 17). Therefore, the second boundary condition was selected for the rest of the simulations due to its simplicity and less solution time. The solution time for the second boundary condition was about 28 minutes, whereas this time was about 40 minutes for the real boundary condition.

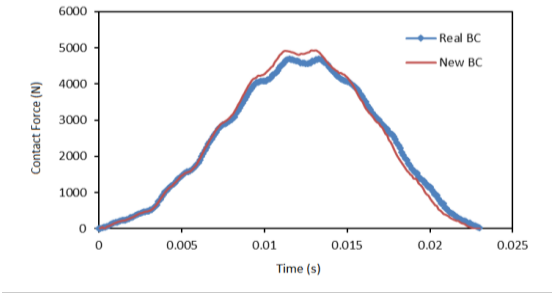

Fig.17
The comparison of the impact response between two different boundary conditions (real and modeled).

4.5 Meshing

The meshing of the structure was significant in terms of reaching correct answers. In this study, 3D elements were used to mesh the sandwich panel. The sweep meshing technique and hexagonal elements were used for the rib, and structured hexagonal elements were used for the shells. All these elements were 3D and were known as the C3D8R element in Abaqus software. The ribs of the grid core and the sandwich panels after meshing are presented in Figs. 18 and 19, respectively. The noteworthy point for meshing the side layers is that a smaller element size was selected for the collision location of the impactor. As a result, the solution accuracy increased, and the solution time of the software was reduced.

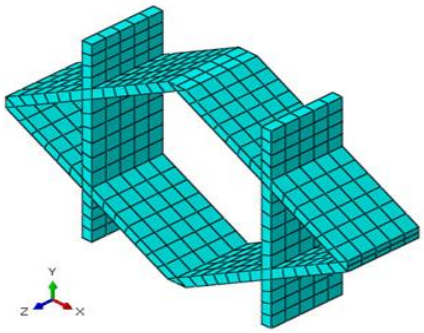

Fig.18
The meshing of the ribs in the grid core of the sandwich panel.

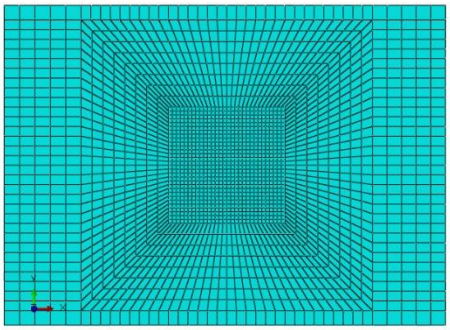

Fig.19
The meshing of the side layers of the sandwich panel and the change in the element size at the impact location.

The suitable number and size of elements are of great importance and play a significant role in obtaining correct results. Thus, achieving suitable element number and type must be investigated in the meshing process. In the present study, the type of elements was selected based on previous studies and the software documentation, and the size of elements was chosen via a mesh convergence investigation. In the graph of Fig. 20, the maximum contact force due to impact was studied with an increase in the number of elements. The point where the graph became horizontal and uniform denotes the minimum number of elements for the correct solution of this geometry.

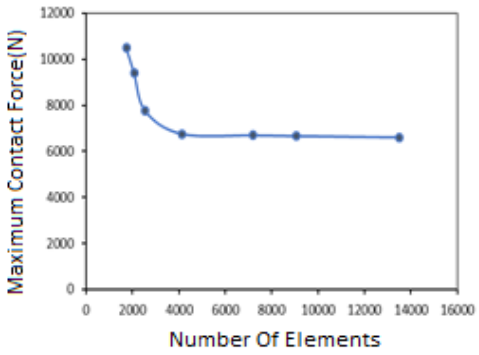

Fig.20
Mesh convergence investigation.

5 RESULTS AND DISCUSSION

5.1 The effect of energy level on the impact response

The impact response of two identical energy levels with different impactor masses and velocities is shown in Fig. 21. Moreover, Fig. 22 displays the energy absorption rate for different initial collision energy levels.

According to the above graph, at low initial energy levels, the energy absorption rate was independent of mass and velocity and was dependent only on the initial energy level. However, with an increase in the initial energy, it was observed that the effect on velocity on the energy absorption rate increases.

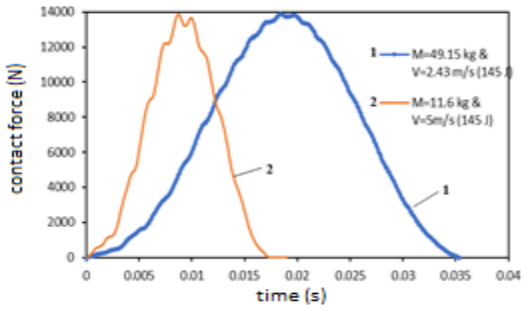

Fig.21
A comparison of the impact response of two identical energy levels with different impactor masses and velocities.

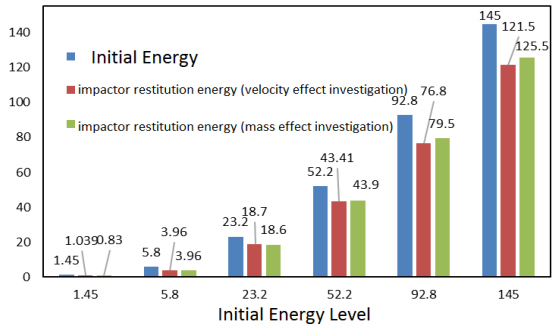

Fig.22
The comparison of the energy absorption rate for different energy levels.

5.2 The effect of the boundary conditions on the impact response

In this section, boundary conditions were applied to the sandwich panel according to Table 4, and the impact response was extracted and is shown in the graph of Fig. 23. In this study, a sandwich panel was selected according to the previous sections, and the impactor was considered to have a mass of 11.6 kg and a velocity of 2.43 m/s.

An investigation of Fig. 23 revealed that the impact response for the first two boundary conditions, representing a cantilever condition, was different from other responses and was in the form of a sine diagram. Furthermore, it was observed that constraining the panel edges increased the rigidity of the panel relative to the simply-supported state, leading to a higher contact force and a shorter contact time.

Table 4
Different modes of boundary conditions applied to the sandwich panel.

1. The displayed side of the sandwich panel is fully constrained at the upper and lower edges (cantilever).	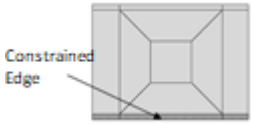
2. The displayed side of the sandwich panel is fully constrained at the upper and lower edges (cantilever).	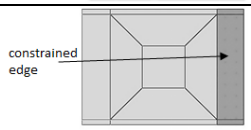
3. The two displayed sides of the sandwich panel are fully constrained at the upper and lower edges. 4. Two sides of the sandwich panel are simply supported.	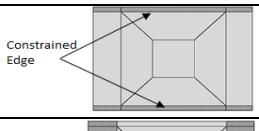
5. The two displayed sides of the sandwich panel are fully constrained. 6. Two sides of the sandwich panel are simply supported.	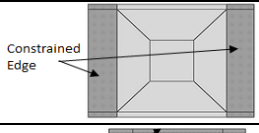
7. The displayed edges of the panel are fully constrained.	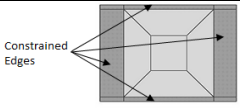

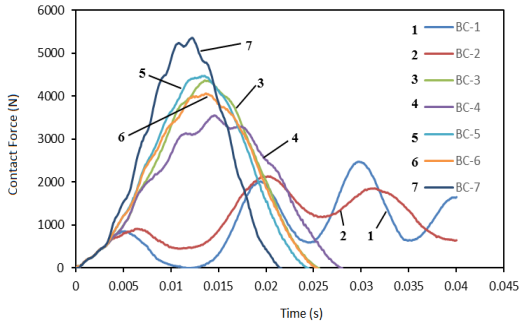

Fig.23
The graph of the numerical solution of the impact on the sandwich panel for different boundary conditions.

5.3 The effect of the impactor shape on the impact response

In this section, the difference between the impact responses of two different impactors was addressed. As shown in Fig. 24, the two impactors were in the form of a sphere and a flat head cylinder with identical masses and impact velocities. The rest of the conditions were as in the previous section.

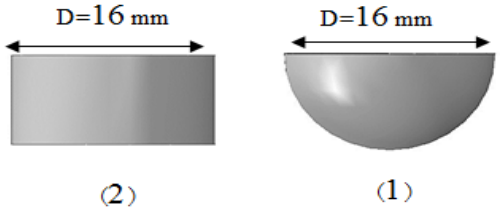

Fig.24
Spherical and flat-head cylindrical impactors.

The impact response and kinetic energy graphs of the sandwich panel without the foam core for two different impactors are presented in Figs. 25 and 26, respectively.

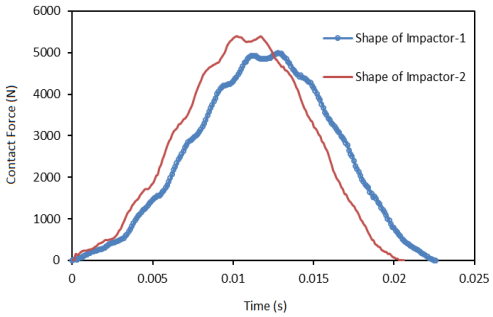

Fig.25
The numerical solution graph of the impact in the foamless sandwich panel for different impactor shapes.

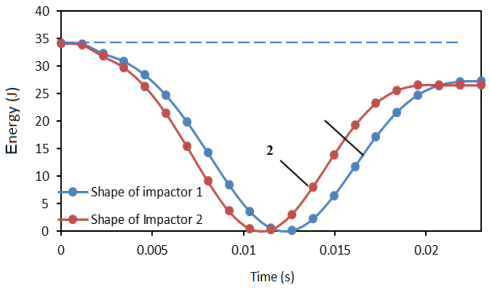

Fig.26
The kinetic energy graph of the foamless sandwich panel for different impactor shapes.

Based on the graph in Fig. 25, the flat shape of the impactor reduced contact time but increased the contact force. Moreover, the energy absorption rate was slightly more for the flat-head impactor than for the spherical impactor.

The impact response and kinetic energy graphs of the sandwich panel with the foam-filled core for two different impactors are presented in Figs. 27 and 28, respectively.

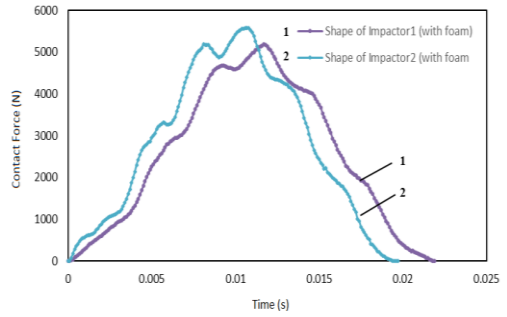

Fig.27
The numerical solution graph of the impact in the sandwich panel with the foam core for different impactor shapes.

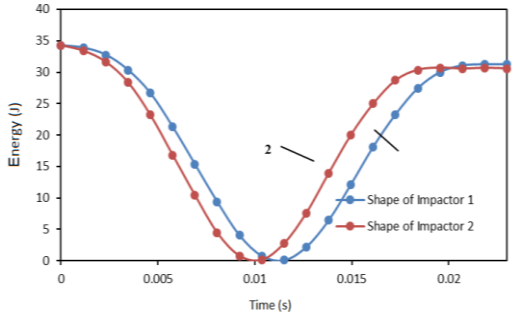

Fig.28
The kinetic energy graph of the sandwich panel with the foam core for different impactor shapes.

As shown in the above figures, the presence of the foam reduced the damage and, hence, the absorption rate. Furthermore, the careful observation of the impact response diagrams of the sandwich panels with and without foam showed that the impact response behaviors for the two impactors were similar, with the difference being only in the contact force and contact time.

5.4 The comparison of different types of sandwich panels against impact

The graph in Fig. 29 shows the impact response for sandwich panels of different materials. This study investigated the impact response of sandwich panels made of glass, Kevlar, and carbon fibers, which are the most common fibers in composite structures.

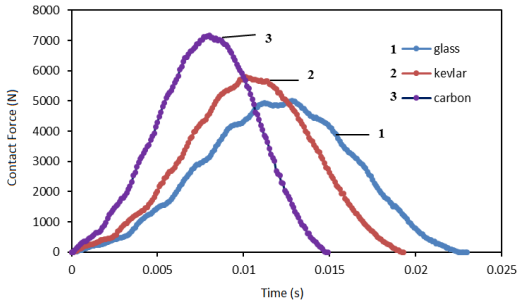

Fig.29
The numerical solution graph of the impact in the foamless sandwich panel for different materials.

As shown in the above figure, the carbon sandwich panel had a higher rigidity than Kevlar and glass ones; thus, the contact force was considerably larger than other panels.

The impact response diagram of the sandwich panel with the foam core was plotted for the three different materials and is shown in Fig. 30. As seen in the figure, the behavior of this panel for different materials was similar to that of the foamless panel, and only the contact force in this state was larger due to the presence of foam.

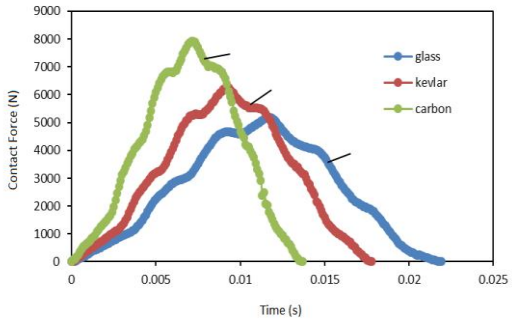

Fig.30
The numerical solution graph of the impact in the sandwich panel with the foam-filled core for different materials.

6 CONCLUSION

In this study, experimental tests and finite element analysis using ABAQUS software were applied to examine low-velocity impact on grid stiffened sandwich panels. In the experimental method, two sandwich panels with grid stiffened core were manufactured and underwent drop weight impact with a hemispherical steel impactor. Also, in the numerical method, the results were compared with 3D elements, and a progressive damage model was applied by employing user defined material subroutines using the finite element method in ABAQUS software. The energy absorption occurred in the structures mainly due to the induced damage in the impact region of the structures. This damage may affect the top face sheets or the ribs within the core of the sandwich panel and the rigidity of the impact position, reducing the visible damaged area in the structure. In general, in phenomena involving impact on composite structures, part of the initial energy of the impactor is used to propagate elastic waves in the structure. If the energy is sufficiently large, part of the energy remains in the structure by damaging the structure, and the rest of the energy causes the impactor to bounce back. Moreover, simply-supported conditions increase the rigidity of the panel, leading to a higher contact force and a shorter contact time. In addition, the flat shape of the impactor reduced contact time but increased the contact force. The energy absorption rate was slightly higher for the flat-head impactor than for the spherical impactor.

REFERENCES

[1] Diamanti K., Soutis C., Hodgkinson J., 2005, Non-destructive inspection of sandwich and repaired composite laminated structures, *Composites Science and Technology* **65**: 2059-2067.

[2] Feraboli P., Kedward K.T., 2006, A new composite structure impact performance assessment program, *Composites Science and Technology* **66**: 1336-1347.

[3] Yang L., Yan Y., Kuang N., 2013, Experimental and numerical investigation of aramid fibre reinforced laminates subjected to low velocity impact, *Polymer Testing* **32**: 1163-1173.

[4] Crupi V., Epasto G., Guglielmino E., 2010, Low-velocity impact strength of sandwich materials, *Journal of Sandwich Structures and Materials* **13**(4): 409-426.

[5] Wang J., Waas A.M., Wang H., 2013, Experimental and numerical study on the low-velocity impact behavior of foam-core sandwich panels, *Composite Structures* **96**: 298-311.

[6] Zhang G., Wang B., Ma L., Wu L., Pan S., Yang J., 2014, Energy absorption and low velocity impact response of polyurethane foam filled pyramidal lattice core sandwich panels, *Composite Structures* **108**: 304-310.

[7] Soroush M., Davar A., Khalili S., 2010, Study of the effect of low velocity impact parameters on the impact response of a multilayer composite plate, *10th Conference of the Iranian Aerospace Association*.

[8] Nasirzadeh R., Sabet A.R., 2014, Study of foam density variations in composite sandwich panels under high velocity impact loading, *International Journal of Impact Engineering* **63**: 129-139.

[9] Buragohain M., Velmurugan R., 2011, Study of filament wound grid-stiffened composite cylindrical structures, *Composite Structures* **93**: 1031-1038.

[10] Hashin Z., 1980, Failure criteria for unidirectional fiber composites, *Journal of Applied Mechanics* **47**: 329-334.

[11] Azarafza R., Davar A., Mahmoodi A., 2017, Three-point bending test of metal and composite sandwich panels with grid stiffened core, *Journal of Science and Technology of Composites* **3**(4): 377-388.

[12] Malekzadeh-Fard K., Azarnia A.H., Zolghadr N., 2018, Analytical modeling to predict dynamic response of Fiber-Metal Laminated Panel subjected to low velocity impact, *Journal of Science and Technology of Composites* **5**(3): 331-342.

[13] Aryal B., Morozov E.V., Wang H., Shankar K., Hazell P.J., Escobedo-Diaz J.P., 2019, Effects of impact energy, velocity, and impactor mass on the damage induced in composite laminates and sandwich panels, *Composite Structures* **226**: 111284.
[14] Zhu Y., Sun Y., 2020, Dynamic response of foam core sandwich panel with composite facesheets during low-velocity impact and penetration, *International Journal of Impact Engineering* **139**: 103508.
[15] Najafi M., Eslami-Farsani R., 2021, Design and characterization of a multilayered hybrid cored-sandwich panel stiffened by thin-walled lattice structure, *Thin-Walled Structures* **161**: 107514.